Electrochemical Sensors Based on Metal-Porous Carbon Nanozymes for Dopamine, Uric Acid and Furazolidone

Jianhui Xiong, Yuxi Yang, Linyu Wang, Shouhui Chen, Yan Du * and Yonghai Song *

College of Chemistry and Chemical Engineering, Jiangxi Normal University,

99 Ziyang Avenue, Nanchang 330022, China.

Materials and reagents

1,3,5-Tris(4-aminophenyl)benzene (TAPB) and 2,6-dihydroxynaphthalene-1,5-diformaldehyde (DHNDA) were purchased from Jilin Chinese Academy of Sciences-Yanshen Technology Co., Ltd. (Changchun, China). Dopamine (DA), uric acid (UA) and furazolidone (FZ), acetic acid ($C_2H_4O_2$), 1,2-dichlorobenzene, 1-butanol, tetrahydrofuran, acetone, $Cu(NO_3)_2 \cdot 6H_2O$, $Fe(NO_3)_3 \cdot 9H_2O$, $Co(NO_3)_2 \cdot 6H_2O$ and $Ni(NO_3)_2 \cdot 6H_2O$ were purchased from Aladdin Co., LTD. (Shanghai, China). $Na_2HPO_4 \cdot 12H_2O$, $NaH_2PO_4 \cdot 2H_2O$, ethanol and other chemical substances were purchased from Beijing Chemical Reagent Factory (Beijing, China). A phosphate buffer (0.2 M PBS) was made from 0.2 M dibasic sodium phosphate solution and 0.2 M sodium dihydrogen phosphate solution. All reagents were analytically pure and were not further purified and used directly. All solution was prepared with ultrapure water, and the ultrapure water purification system is the Millipore - Q purified ($\rho \geq 18.2$ MΩ cm^{-1}).

Instruments

JEM-2010 (HR) was used for obtaining transmission electron microscopy image (TEM). Fourier transform infrared spectroscopy (FTIR) was recorded on model Perkin-Elmer Spectrome 100 spectrometer (Perkin-Elmer Company, USA). N_2 adsorption/desorption isotherm measurement was operated using a BELSORP-mini II instrument under the liquid nitrogen temperature (77 K). X-ray photoelectron spectroscopy was taken using the ESCA-LAB-MKII, with Al Kα as the excitation source, and C1s (284.6 eV) as the reference line. SDT 2960 was used for obtaining the instrument model of the thermogravimetric analysis (TGA), the heating rate was 10 °C min^{-1}, and the test was performed under a nitrogen atmosphere. Powder X-ray diffraction (XRD) analysis was performed on a D/Max 2500 V/PC X-ray powder diffractometer using Cu Kα radiation range from 2° to 35°

with scanning step controlled 1°/min. All electrochemical measurements were performed on a CHI 760D electrochemical workstation (Shanghai, China) with a conventional three-electrode system including COF_{TD}/GCE, CN/GCE and MNPs/GCE (M=Cu, Fe, Co, Ni) modified electrode as the working electrodes, a platinum wire as the auxiliary electrode and a saturated calomel electrode (SCE, saturated KCl) as the reference electrode. Cyclic voltammetry (CVs) and electrochemical impedance spectroscopy (EIS) were performed in a 0.1 M KCl solution containing 5.0 mM $Fe(CN)_6^{3-/4-}$, the frequency range is 0.01-100 KHz, and the voltage was the open circuit voltage. AC impedance was used to analyze the electron transmission rate and the interface state of ion transmission at various stages. The differential pulse voltammetry (DPV) test was performed in 0.2 M N_2-statured PBS (pH=7).
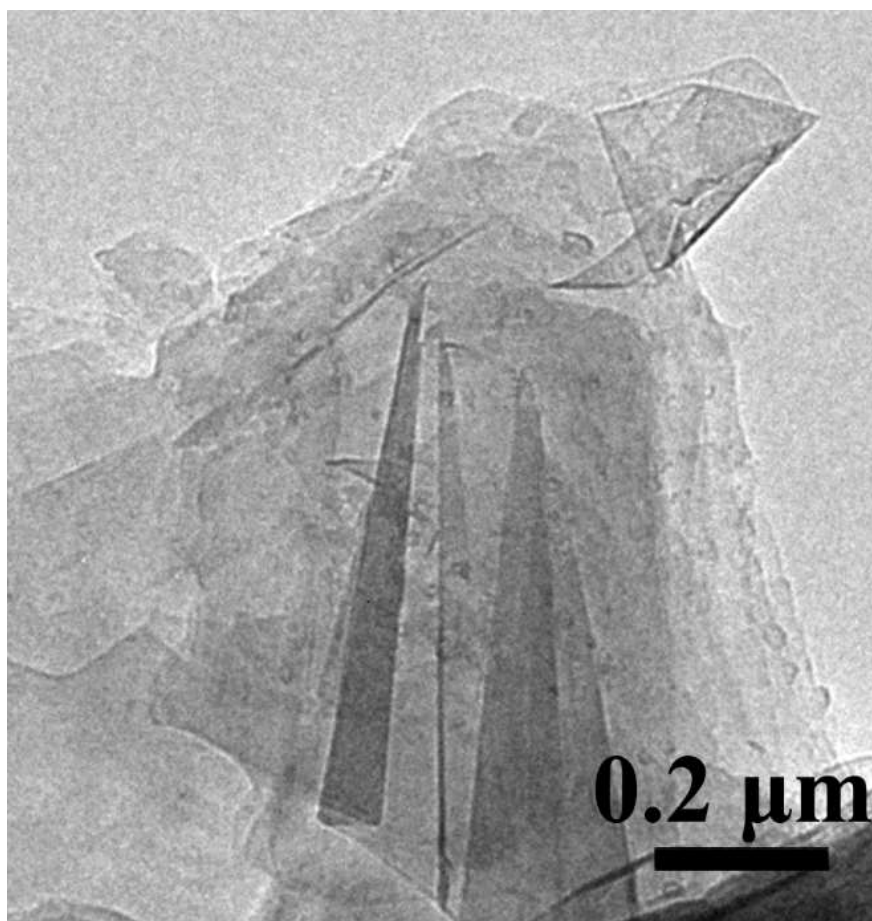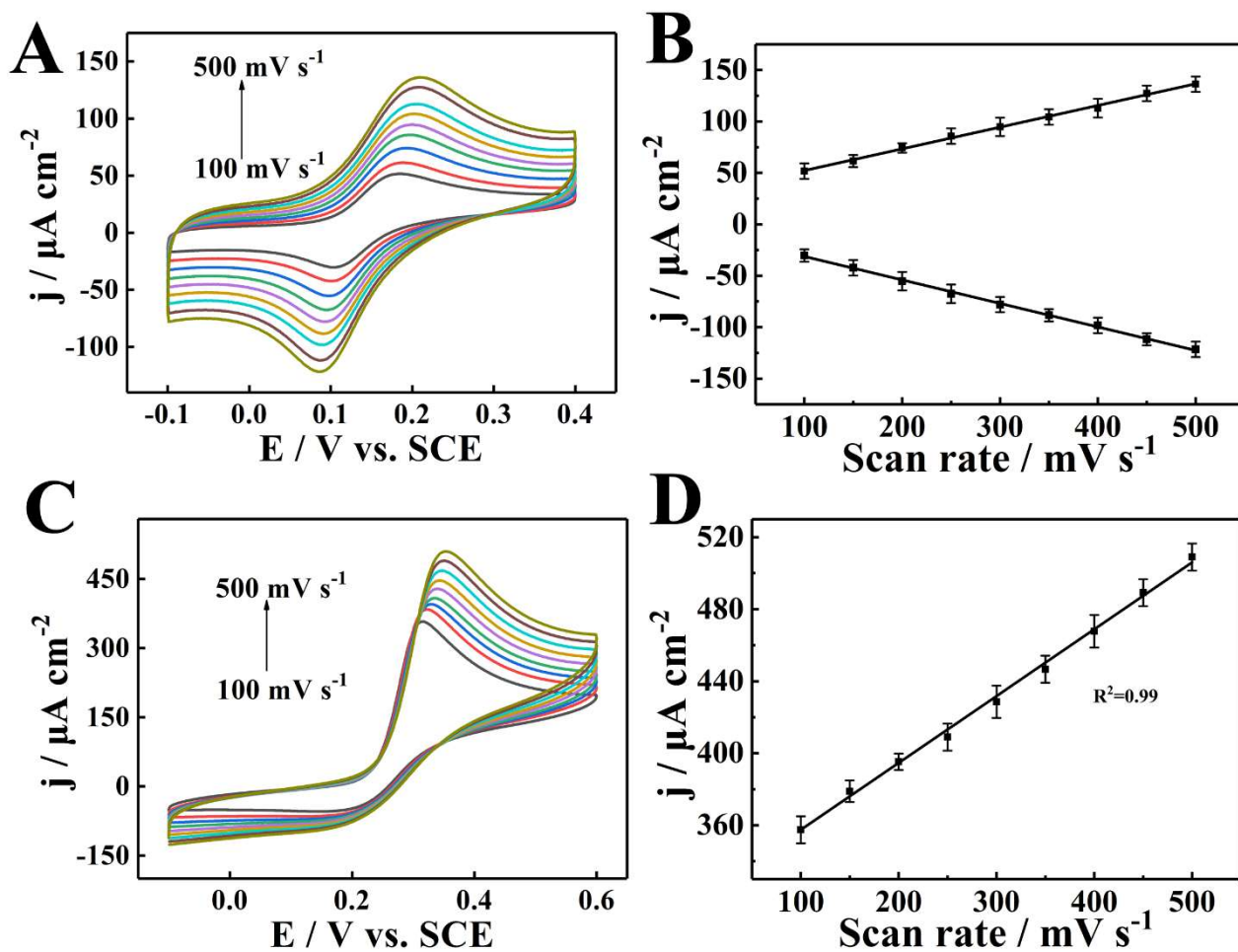
Figure S1. TEM image of CN.

Figure S2. CVs of CuNPs/CN/GCE at different scan rates from 100 mV s^{-1} to 500 mV s^{-1} in 0.2 M

N$_2$-statured PBS (pH=7.0) to the detection of DA (**A**) and UA (**C**). Fitting curve between current

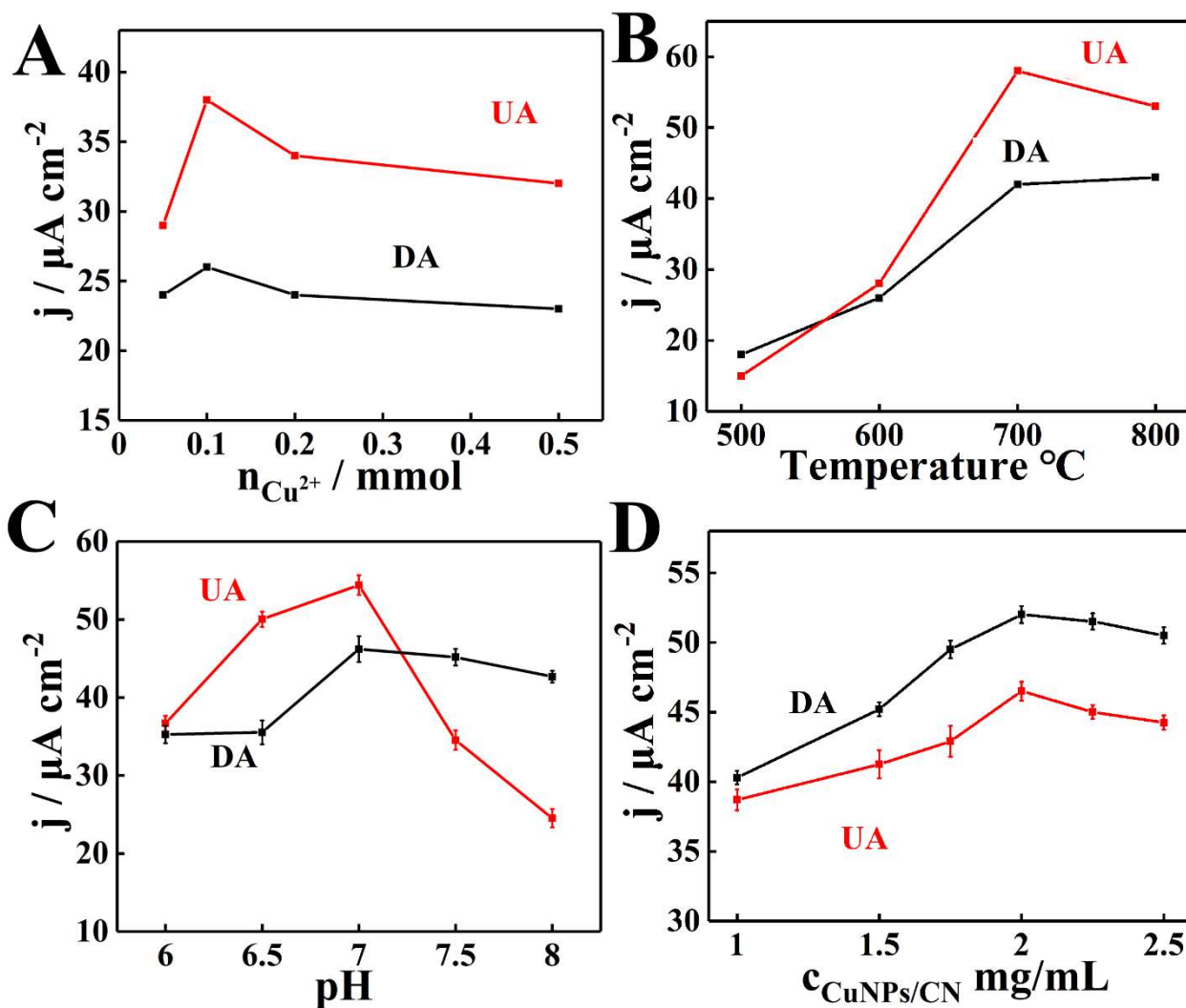density and the concentration of DA (**B**), UA (**D**)

Figure S3. (**A**) The plot of peak current density versus Cu^{2+} concentrations. (**B**) The plot of peak current density versus different temperatures of carbonization. (**C**) The plot of peak current density versus different pH. (**D**) The plot of peak current density versus different concentrations of CuNPs/CN.
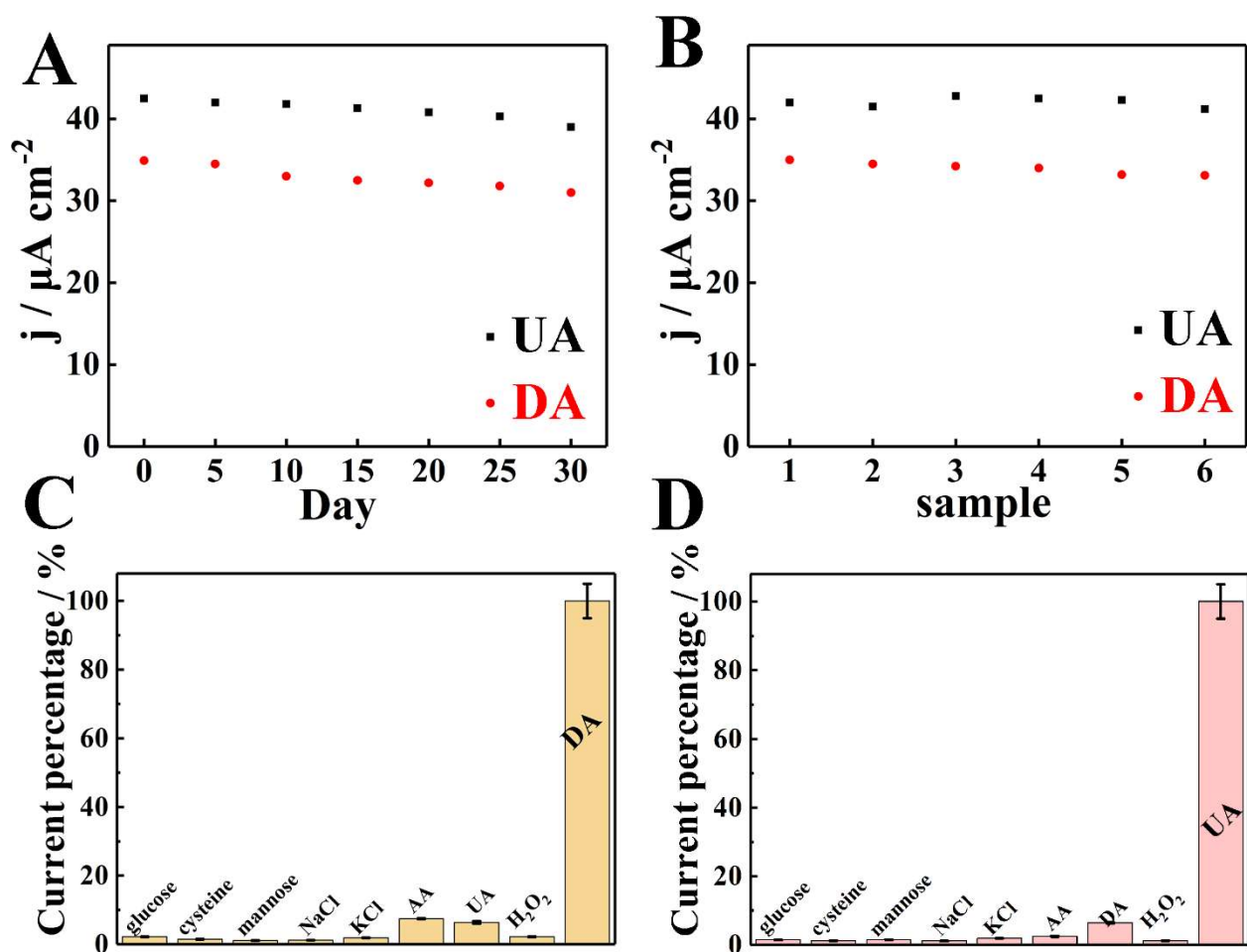
Figure S4. (**A**) Stability of the CuNPs/CN/GCE for DA and UA detection. (**B**) Reproducibility of the CuNPs/CN/GCE for DA and UA detection. (**C,D**) Selectivity of the CuNPs/CN/GCE for DA and UA detection.
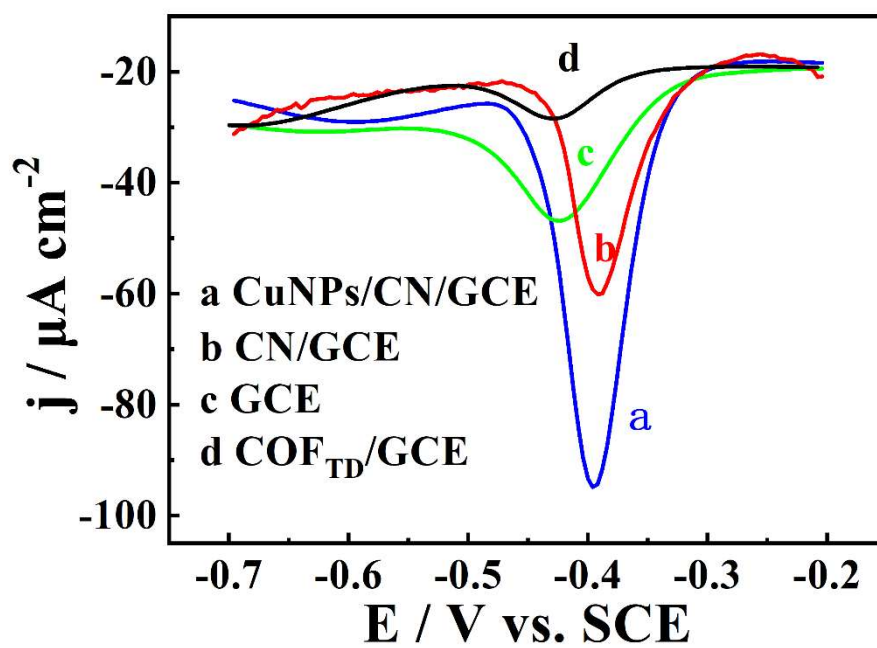
Figure S5. DPV of CuNPs/CN/GCE, CN/GCE, GCE, COF$_{TD}$/GCE in 0.2 M PBS solution (pH=7) containing FZ.
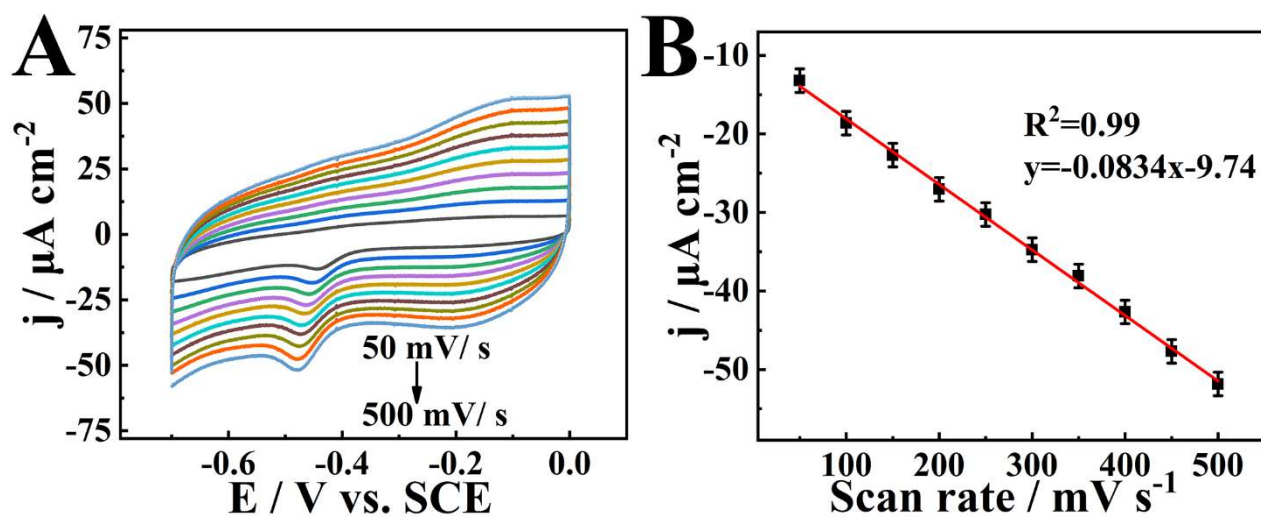
Figure S6. (**A**) CVs of CuNPs/CN/GCE at different scan rates from 50 mV s^{-1} to 500 mV s^{-1} in 0.2 M N$_2$-statured PBS (pH=7.0) to the detection of FZ. (**B**) Fitting curve between current density and different scan rates.
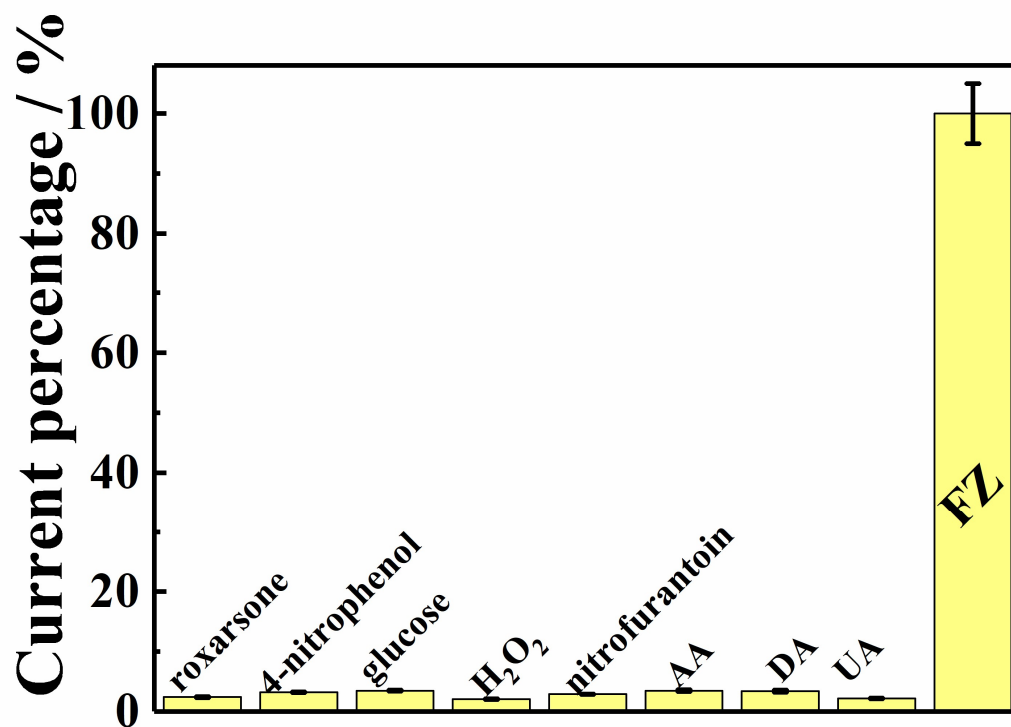
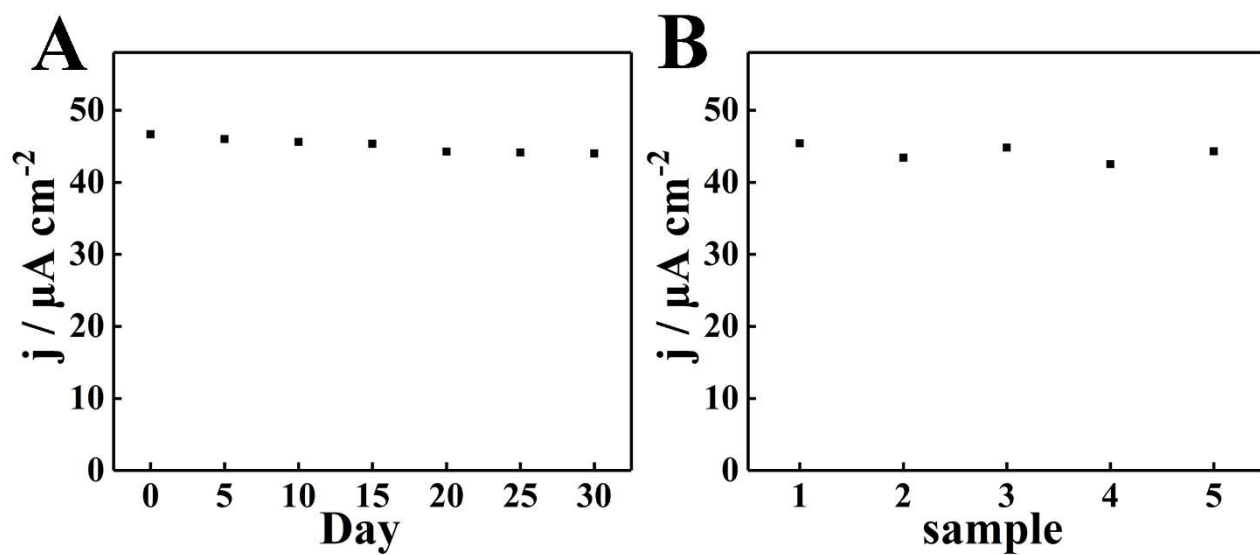**Figure S7.** Selectivity of the CuNPs/CN/GCE for FZ detection.

Figure S8. (**A**) Stability of the CuNPs/CN/GCE for FZ detection. (**B**) Reproducibility of the CuNPs/CN/GCE for FZ detection.

Table S1. Comparison of the sensor based on based on MNPs/CN nanozymes to other DA and UA sensors.

Electrode	Linear range (μM)	LOD(μM)	Reference
HNP-PtTi alloy	DA: 25-50	2.08	[1]
	UA: 120-230	5.7	
Au-Cu$_2$O/rGO	DA: 10-90	3.9	[2]
	UA: 100-900	6.5	
pCu$_2$O NS-rGO	DA:0.05-109.0	0.015	[3]
	UA: 1.0-1380.0	0.122	
g-C$_3$N$_4$/Co	DA: 2-400	0.4	[4]
	UA: 1-1000	0.4	
h-BN	DA: 10-300	5	[5]
	UA: 10-500	4	
Au NPs@3D GR/ITO	DA: 0.1-5	0.1	[6]
	DA: 5-60	-	
NCCNPs800/GCE	DA:2-69.5	0.34	[7]
	UA:5-192	0.98	
CuNPs/CN/GCE	DA:10-200	0.042	This work
	UA:100-1100	0.12	
FeNPs/CN/GCE	DA:0.1-200	0.035	This work
	UA:0.5-900	0.145	
CoNPs/CN/GCE	DA: 0.15-250	0.042	This work
	UA: 0.25-900	0.077	
NiNPs/CN/GCE	DA: 0.15-250	0.052	This work
	UA: 0.4-800	0.125	

Table S2. Comparison of the sensor based on based on MNPs/CN nanozymes to other FZ sensors.

Electrode	Linear range (μM)	LOD (nM)	Reference
COF@NH$_2$-CNT	0.2-100	77.5	[8]
SnS$_2$-SnO$_2$/graphene/GCE	0.015–190.5	1.42	[9]
Gr/Au/GCE	1-674	64.00	[10]
PAR/GCE	50-200	340	[11]
NiFe$_2$O$_4$/rGO	0.1-150	50	[12]
h-BN/HNTs	0.009-173.0	1	[13]
CuNPs/CN/GCE	0.06-200	20.1	This work

References

[1] Zhao D, Yu G, Tian K, et al. A highly sensitive and stable electrochemical sensor for simultaneous detection towards ascorbic acid, dopamine, and uric acid based on the hierarchical nanoporous PtTi alloy [J]. Biosens. Bioelectron, 2016, 82:119-126.

[2] Aparna T K, Sivasubramanian R, Dar M A. One-pot synthesis of Au-Cu$_2$O/rGO nanocomposite based electrochemical sensor for selective and simultaneous detection of dopamine and uric acid [J]. J. Alloy Compd, 2018, 741: 1130-1141.

[3] Mei L-P, Feng J-J, Wu L, et al. A glassy carbon electrode modified with porous Cu$_2$O nanospheres on reduced graphene oxide support for simultaneous sensing of uric acid and dopamine with high selectivity over ascorbic acid [J]. Microchim Acta, 2016, 183(6): 2039-2046.

[4] Wang M, Zhang M, Zhu J, et al. G-C$_3$N$_4$/Co nanohybrids for ultra-sensitive simultaneous detection of uric acid and dopamine [J]. ChemElectroChem, 2020, 7(6): 1373-1377.

[5] Bi Y-S, Liu B, Liu X-Y, et al. A h-BCN for electrochemical sensor of dopamine and uric acid [J]. J Nanomater, 2020, 2020: 1-9.

[6] Wang Z, Yue H Y, Huang S, et al. Gold nanoparticles anchored onto three-dimensional graphene: simultaneous voltammetric determination of dopamine and uric acid [J]. Mikrochim Acta, 2019, 186(8): 573.

[7] Guo H, Wang M, Zhao L, et al. The effect of Co and N of porous carbon-based materials fabricated via sacrificial templates MOFs on improving DA and UA electrochemical detection [J]. Microporous Mesoporous Mater, 2018, 263: 21-27.

[8] Sun Y, Waterhouse G I N, Xu L, et al. Three-dimensional electrochemical sensor with covalent organic framework decorated carbon nanotubes signal amplification for the detection of furazolidone [J]. Sens Actuators B, 2020, 321: 128501.

[9] Amalraj A J J, Umesh N M, Wang S F. Synthesis of core-shell-like structure SnS_2-SnO_2 integrated with graphene nanosheets for the electrochemical detection of furazolidone drug in furoxone tablet [J]. J Mol Liq, 2020, 313: 113554.

[10] He B S, Du G A. A simple and sensitive electrochemical detection of furazolidone based on an Au nanoparticle functionalized graphene modified electrode [J]. Anal Methods, 2017, 9(30): 4341-4348.

[11] Chen C X, Chen W, Jiang J L, et al. Nitrofuran determination in aquaculture water by using poly-alizarin red-modified electrode [J]. J Electrochem Soc, 2019, 166(10): H425-H432.

[12] Ensafi A A, Zandi-Atashbar N, Gorgabi-Khorzoughi M, et al. Nickel-ferrite oxide decorated on reduced graphene oxide, an efficient and selective electrochemical sensor for detection of furazolidone [J]. IEEE Sens J, 2019, 19(14): 5396-5403.

[13] Kokulnathan T, Wang T-J, Thangapandian M, et al. Synthesis and characterization of hexagonal boron nitride/halloysite nanotubes nanocomposite for electrochemical detection of furazolidone [J]. Appl Clay Sci, 2020, 187: 105483.